

Studies on physical properties of nanostructured ZnO doped Bi-2223 superconductors

Indu Verma*, Ritesh Kumar and Nidhi Verma

Departments of Physics, University of Lucknow, Lucknow 226007, India

*Corresponding author. Tel: (+91) 7376807397; Fax: (+91) 522-2740467; E-mail: sheeluvermaindu@gmail.com

Received: 08 Nov 2011, Revised: 22 March 2012 and Accepted: 25 March 2012

ABSTRACT

Samples of $(\text{Bi,Pb})_2\text{Sr}_2\text{Ca}_2\text{Cu}_{3-x}\text{Zn}_x\text{O}_{10+\delta}$ (Bi-2223, $x=0.0$ to 0.30) were synthesized by solid-state reaction route. We carefully synthesized these compounds and characterized them for phase formation, structural/microstructural, electrical and magnetic measurements. The phase identification /gross structural characteristics of synthesized (HTSC) materials explored through powder x-ray diffractometer reveals that all the samples crystallize in orthorhombic structure with lattice parameters $a = 0.5405$ nm, $b = 0.5422$ nm and $c = 3.7063$ nm up to Zn concentration of $x = 0.30$. The critical temperature (T_c) measured by standard four probe method has been found to depress from 108 K to 92 K and transport current density (J_c) has been increased from Zn content (x) increases from 0.00 to 0.30. The surface morphology/topography explored by scanning electron and atomic force microscopy (SEM & AFM) shows that microspheres/ nanospheres like structures, voids, grains size & porosity on the surface of the Zn doped Bi-2223 sample increases as the Zn concentration increases. From the magnetic properties measurement (M-H), the ac susceptibility (χ_{ac}) and the lower (H_{c1}) & upper (H_{c2}) critical magnetic field were observed at 10 K from the M-H loop respectively. Copyright © 2012 VBRI Press.

Keywords: Melt textured cuprates; vortex flux pinning; magnetic measurements; critical magnetic fields.



Indu Verma has received her B.Sc. degree in 2004 from University of Lucknow and M.Sc. degree in 2006 from Dr. R.M.L. Avadh University, Faizabad, Uttar Pradesh, India. Currently she is pursuing Postdoc Women's fellowship from UGC, Delhi. She has published more than fifteen research papers on Synthesis of high T_c superconductors. Her research topic is "Synthesis and characterization of Bi-based high temperature superconductor". His current interests of

research are in synthesis of nanomaterials and their applications as physical, chemical and optical sensors.



Nidhi Verma has received her B.Sc. degree in 2006 from University of Lucknow and M.Sc. degree in 2008 from Dr. R.M.L. Avadh University, Faizabad, Uttar Pradesh, India. Currently she is a Ph. D. student at Nanomaterials & Sensors Research Laboratory, Department of Physics, University of Lucknow, Lucknow under the supervision of Dr. B.C. Yadav. Her research topic is "Design and Fabrication of Opto-Electronic Humidity Sensor based on Nanocomposite Metal Oxides".



Ritesh Kumar has received his B. Sc. and M. Sc. Degrees from Lucknow University, Lucknow, India. He obtained his Ph.D. degree in year 2011 from Department of Physics, University of Lucknow, and Uttar Pradesh, India. Currently he is Assistant Professor in the Department of Physics in the Maulana Azad National Urdu University, Bangalore. He has published more than twenty research papers on Synthesis of Nanomaterials and Sensor Applications. His research topic is

synthesis of nanomaterials and their applications as physical, chemical and optical sensors

Introduction

High temperature superconductor (HTSC) is the short coherence length (0.3–2.0 nm), which is several orders of magnitude shorter than that of the conventional superconductor (400 to 10 000 Å) because by combining the two dimensional nature of the structure together with electron phonon coupling mechanism, the electron-phonon coupling was found to be 10–100 times smaller than conventional superconductors [1]. HTSC materials are their successful application which depends on the fabrication of long length conductors, such as wires and tapes with high current carrying capacity ($J_c \sim 10^4$ A/cm²). One of the methods used to improve the current carrying capacity is to

use fabricate nanoparticles dispersed HTSC tapes [2-3]. The nanoparticles of about 50-100 nm size have been employed to enhance the properties of the Bi-based and Tl-based tapes [4]. The magnetic properties measurements of Zn and Ga-doped sintered Bi-based compounds were carried out in a 40 T high-field facility [5]. The critical current density and the flux pinning force of the Bi-series oxide superconductors were calculated using Bean's critical state model [6]. It is found that both the critical current density and the flux pinning force of the Zn-doped oxide compounds are decreased slightly with increasing Zn content. However, the critical current density and the flux pinning force of the Ga-doped oxide superconductors diminish significantly with enhancement of dopant content. It seems that the superconductivity of Bi-series superconductors is much more severely destroyed by a trivalent dopant than by a divalent one [7]. They argue that the scanning tunneling microscope (STM) images of resonant states generated by doping Zn or Ni impurities into CuO planes of Bi-Sr-Ca-Sr-O (BSCCO) are the result of quantum interference of the impurity signal coming from several distinct paths. The impurities of the nano size are important because these particles can interact with the flux, which is about of the same size. The effect of the substitution of Mn, Fe, and Zn for Cu on the superconducting properties of $(\text{Bi, Pb})_2\text{Sr}_2\text{Ca}_2\text{Cu}_{3-x}\text{Mn}_x\text{O}_{10+\delta}$ ($0 \leq x \leq 0.5$) have also been investigated by means of X-ray diffraction, DC magnetic susceptibility and electrical resistivity measurements. The temperature at which the resistivity is zero decreases monotonically with x in the region $x \leq 0.07$ for the Zn and Fe- doped samples. The Fe-doped samples with $x > 0.1$ are not superconducting while the corresponding Zn-doped samples are superconducting with the amount of the Bi-2212 phase increasing with increasing Zn concentration. The effect of Mn doping on the superconductivity is less than that of Zn and Fe. There is evidence of weak links between superconducting grains. Pair-breaking effects due to the effect of doping seem to give a satisfactory explanation of the reduction in T_c . The results for the low dopant concentrations lead to the conclusion that local disorder rather than magnetism is the important factor for the suppression of superconductivity in the samples [8]. Using scanning tunneling spectroscopy (STS), we report the correlation between spatial gap in homogeneity and the zinc (Zn) impurity resonance in single crystals of $\text{Bi}_2\text{Sr}_2\text{Ca}(\text{Cu}_{1-x}\text{Zn}_x)_2\text{O}_{8+\delta}$ with different carrier (hole) concentrations (p) at a fixed Zn concentration ($x \leq 0.5$ % per Cu atom). In all the samples, the impurity resonance lies only in the region where the gap value is less than 60 meV. Also the number of Zn resonance sites drastically decreases with decreasing p , in spite of the fixed x . These experimental results lead us to a conclusion that the Zn impurity resonance does not appear in the large gap region although the Zn impurity evidently resides in this region [9]. High temperature superconductors are also known for their strong anisotropic properties, very low charge density, extremely short coherence length ($\xi \sim 2\text{-}30 \text{ \AA}$) and large penetration depth ($\lambda \sim 1650 \text{ \AA}$ for a-b plane & 8000 \AA for c-plane). $\text{Bi}_2\text{Sr}_2\text{Ca}_2\text{Cu}_3\text{O}_{10}$ tapes and cables of hundreds meters are available from several manufacturers [10-12]. Considerable progress has also been achieved in processing tapes containing several filaments embedded in

a silver matrix ("multifilamentary tapes"). The main advantages of multifilamentary tapes as compared to monofilamentary ones are: (i) a reduction of AC losses [13-16], (ii) an improved current distribution uniformity [16] and (iii) better mechanical properties.

Hence aim of the present paper is to study the effect of the substitution/addition of nonmetallic element such as Zn with different doping concentrations ($0.0 \leq x \leq 0.30$) at Cu-sites in Bi-2223 $(\text{Bi,Pb})_2\text{Sr}_2\text{Ca}_2\text{Cu}_{3-x}\text{Mn}_x\text{O}_{10+\delta}$, on the physical properties (T_c , J_c , H_c etc) and structural /microstructural properties.

Experimental

$\text{Bi}_{1.6}\text{Pb}_{0.4}\text{Sr}_2\text{Ca}_2\text{Cu}_3\text{O}_{10+\delta}$ (Bi, Pb)-2223 samples were prepared by a conventional solid -state reaction method. In brief, the powders of high grade purity Bi_2O_3 (99.99%, Alfa Aesar), PbO (99.99%, Alfa Aesar), SrCO_3 (99.9%, Alfa Aesar), CaCO_3 (99.9%, Alfa Aesar), ZnO (99.99%, Alfa Aesar) and CuO (99.99%, Alfa Aesar) were mixed and ground in an agate mortar pestle, put in cylindrical boats and calcined at 820°C for 24 hrs in air. After that it was mixed and pressed into pellets. Finally, the pellets (samples) were sintered at 848°C for 34 hrs and slowly furnace cooled to room temperature. The homogeneous powder thus formed was converted into the form of pellets before sintering. For this we employed the most widely used technique i.e. dry pressing, which consists of filling a die with powder and pressing at 400 Kg/cm^2 into a circular shape. The nominal composition Bi-2223 samples were sintered in air very near to melting point ($\sim 848^\circ\text{C}$) for 34 hrs and then cooled slowly down to room temperature ($\sim 30^\circ\text{C}$). The heat treatment schedule for Bi-2223 pellets in programmable temperature controlled silicon carbide (SiC) furnace is shown in Fig. 1.

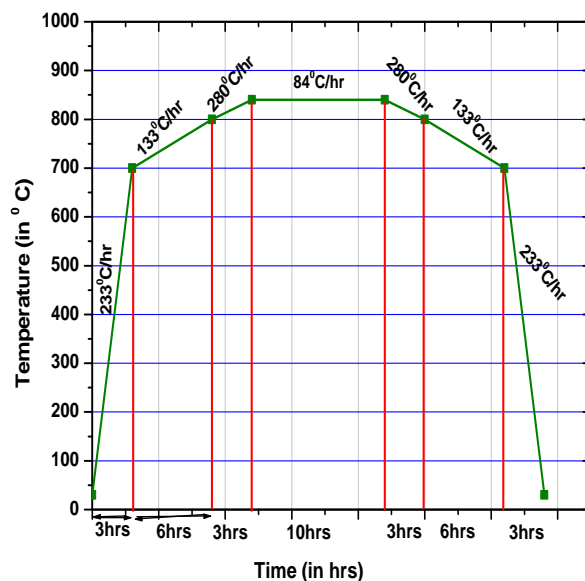


Fig. 1. The heat treatment schedule for Zn-doped Bi-2223 (In programmable temperature controlled silicon carbide (SiC) furnace).

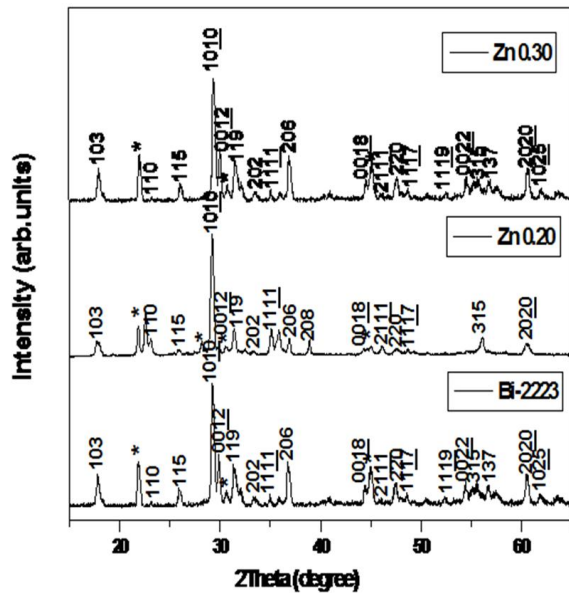


Fig. 2. Powder X-ray diffractogram of $\text{Bi}_2\text{Sr}_2\text{Ca}_2\text{Cu}_{3-x}\text{Zn}_x\text{O}_{10+\delta}$ with $x = 0.0, 0.20$ and 0.30 and (*) sign indicates the presence of other impurity phases.

Results and discussion

Fig. 2 shows the representative X-ray powder diffraction pattern for various nominal compositions of $(\text{Bi}, \text{Pb})_2\text{Sr}_2\text{Ca}_{n-1}\text{Cu}_{n-x}\text{Zn}_x\text{O}_{10+\delta}$ ($n = 3$) with $x = 0.0$ to 0.30 . Besides Bi-2223 as major phase, some other minority phases indexed by starred (*) sign were also found. The crystal structure of Bi-2223 is found to be orthorhombic with $a = 5.4048 \text{ \AA}$, $b = 5.4358 \text{ \AA}$ and $c = 37.0634 \text{ \AA}$ for Zn substitution upto $x = 0.30$. It is also observed that the maximum number of peaks of Bi-2223 phase are present for Zn substituted ($x = 0.1$) samples. The presence of impurity phases is significant in other Zn substituted Bi-2223 samples of higher Zn-concentrations. As the zinc content increases, other peaks appear in the x-ray diffractograms which are Zn-rich compounds due to the easier formation of Zn-Cu clusters. These starred peaks were identified as CaZnO_2 , CuZnO_2 and unreacted Bi_2O_3 . These Zn-rich compounds reduce the amount of Bi-2223 phase and enhance the formation of Bi-2212 phase.

One of the most important properties of high transition temperature in ceramic superconductors is their grained structure. These grained structures can be easily examined by the SEM photographs. In the samples, all of the grains headed randomly and grain boundaries seem to be in touch with each other as to make weak bonds. Also, this is one of the most characteristic properties of the high-temperature superconductors. The SEM images of the surfaces of as synthesized samples are shown in Fig. 3.

One of the most important properties of high transition temperature in ceramic superconductors is their weakly bonded granular structures. The size of pores or voids decreases with increasing Zn concentration. The crystalline behavior is observed excellent in Zn substituted Bi-2223 for $x = 0.30$. The interconnectivity of the grains as appeared from their compactness increases as the Zn-concentration increases.

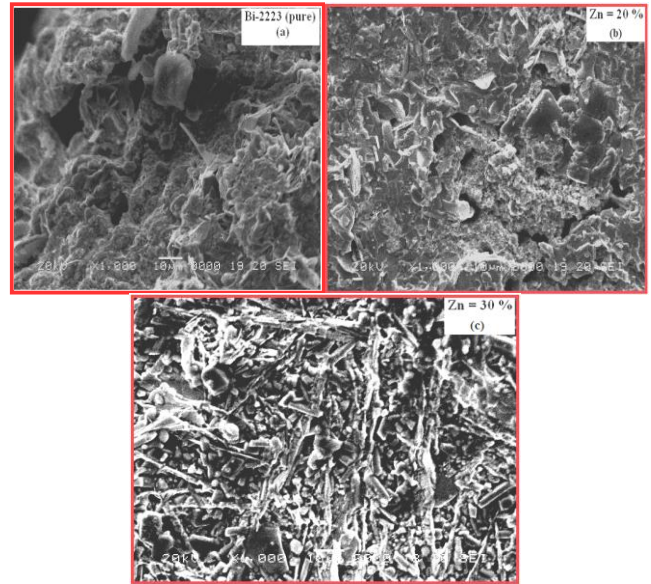


Fig. 3. Scanning electron micrograph of Zn doped $\text{Bi}_2\text{Sr}_2\text{Ca}_2\text{Cu}_{3-x}\text{Zn}_x\text{O}_{10+\delta}$ with $x = 0.0$ to 0.30 .

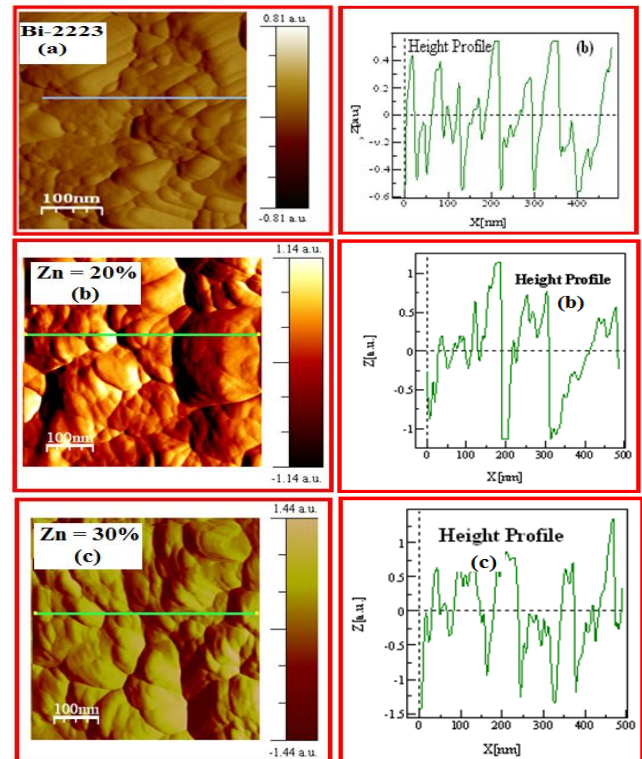


Fig. 4. Two dimensional (2D) AFM images (shown in left) of Zn doped Bi-2223 melt textured (sintered at 848°C , very near to melting temperature of the pellets for 24 hrs) in contact mode and air and its corresponding height profile curves (shown in right).

The two-dimensional AFM image appears as a nanosphere, like structure on the surface as shown in Fig. 4 (a to c). The most pronounced difference in the two layers of oxide is around 40.67 nm . It is noted that fluctuation in the scan profile in the upper layer as well as in the lower layer is due to changes from one grain to another grain of the oxides. The formation of the humps in some places could be clearly seen, which is due to formation of an oxide

layer with different thickness depending on the chemical composition of phases.

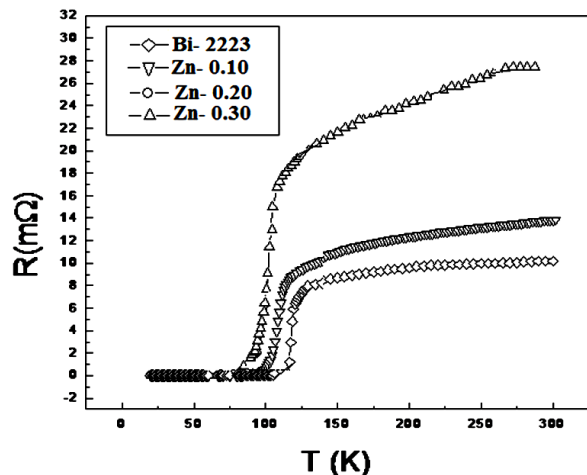


Fig. 5. Temperature dependence of electrical resistance for $\text{Bi}_2\text{Sr}_2\text{Ca}_2\text{Cu}_3\text{-xZn}_x\text{O}_{10+\delta}$ with $x = 0.0$ to 0.30 .

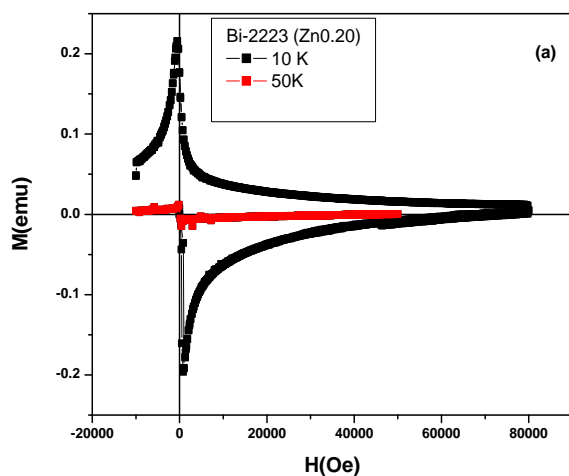


Fig. 6. (a) Shows the hysteresis M-H loops for Bi-2223 with Zn = 0.20 doped high temperature Superconductor at 10K & 50K.

The temperature dependence of electrical resistance- $R(T)$ is measured by four-probe method for pure and Zn-doped $\text{Bi}_2\text{Sr}_2\text{Ca}_2\text{Cu}_3\text{-xZn}_x\text{O}_{10+\delta}$ with $x = 0.0$ to 0.30 and results are shown in Fig. 5 in various applied external magnetic fields. The transition temperature (T_c) (defined as the temperature at which dR/dT has a maximum) was determined from electrical resistance measurements. As the Zn content increases from 0.0 to 0.30 , the transition temperature decreases from 108 K to 90 K for Bi-2223 samples.

It can be seen from the table that transition width increases as Zn concentration increases from $x = 0$ to $x = 0.30$. This is due to the fact that during synthesis process impurity phases are formed easily in case Zn-doped Bi-2223 samples.

Fig. 6 (a) shows a typical M-H loops from zero field to the highest applied field of $80,000$ Oe for the Zn doped Bi-2223 sample sintered at 848°C , the temperature very near to the melting of samples. At very low fields, in perfect diamagnetically shielded state, the M-H loop is a reversible straight line with a slope of magnitude equal to the

superconducting volume fraction at that temperature and field. Critical current density (J_c) was calculated following the extended Bean's Critical State model using the formula-

$$J_c = 30 \frac{\Delta M}{d} A / \text{cm}^2$$

Here ΔM (in G) is the difference in the hysteretic magnetization between the curves obtained while increasing and decreasing the magnetic fields ($M = M^+ - M^-$) and,

$$d = [b(1 - \frac{b}{3a})]$$

It is the reduced dimension, where 'a' and 'b' are the planar dimensions (in cm) of the sample with $a > b$. Also in the present study, the sample shows opened loop even at minimum applied field of 0.12 Oe, at temperature of 10 K, indicating the lower critical magnetic field (H_{c1}) of 0.12 Oe. Beyond this field, since the superconducting volume fraction of the weak link region reduces the M-H loop collapses and is reflected as an inflexion in the rate at which the loop area increases with the field. However, since the upper critical magnetic field (H_{c2}) is higher than the lower critical magnetic field (H_{c1}) of Zn doped Bi-2223 sample, the loop does not collapse. The upper critical magnetic field (H_{c2}) of Zn doped Bi-2223 sample is calculated from M-H loops at 10 K and found to be 8.0 Oe. Finally the magnetic susceptibility (χ) and intra-grain critical current density (J_c) of Zn doped Bi-2223 samples were calculated from the formulas i.e. $\chi = \Delta M / \Delta H$ and

$$J_c = 30 \frac{\Delta M}{d} A / \text{cm}^2$$

A cm^{-2} (Bean's model) and were found to be -4.4146×10^{-5} and $4.283 \times 10^5 \text{ A/cm}^2$ respectively.

Conclusion

We have successfully prepared samples of $\text{Bi}_2\text{Sr}_2\text{Ca}_{n-1}\text{Cu}_n\text{-xZn}_x\text{O}_{10+\delta}$ (where $n = 2$ and $x = 0.0$ to 0.30) by solid-state reaction method. The structure of Bi-2223 phases does not change with the substitution of Zn up to $x = 0.30$ but lattice parameters 'a' & 'c' are changed. The lattice parameter 'a' increases with increasing Zn content but 'b' contracts with increasing Zn content. The lattice parameter 'c' does not change with change in Zn content. The contraction of lattice periodicity 'b' may be due to the partial replacement of larger ionic radius of Cu^{2+} ($r = 0.72 \text{ \AA}$) by the smaller ionic radius of Zn^{2+} ($r = 0.60 \text{ \AA}$) whereas elongation in the lattice parameter 'a' may be due to the partial replacement of mixed valent copper (2^+ & 3^+) by Zn^{2+} ions. The surface morphology of Zn-doped Bi-based cuprates exhibits well connected grains, pores and various particle sizes for different amount of doping. In the SEM study, it has been found that the particle size increases with increasing Zn concentration upto 0.30 . The two-dimensional (2D) AFM images of pure and Zn-doped Bi-2223 ($x = 0.0$ to 0.30) melt textured samples (sintered at very near to melting temperature (848°C) for 24 hrs show that the surfaces consists of uniformly distributed nanogranules of different

shapes. It is also observed that the roughness of the samples increased with increasing doping concentration; the roughness is in the range 87.5 nm to 751.6 nm. Transition temperature (T_c) decreases slowly from 108K to 90K in the absence of magnetic field. The suppression in T_c have been found due to following reasons (i) Zn ions (Zn^{+2}) have a full d shell ($3d^{10}$) and are nominally nonmagnetic scatters. (ii) Zn induced a localized moment on neighboring Cu-sites. (iii) Zn^{+2} have a filled d shell ($3d^{10}$) and hence acts as a strong potential scattered for holes in the CuO_2 plane. At very low fields, in perfect diamagnetically shielded state, the M-H loop is a reversible straight line with a slope of magnitude equal to the superconducting volume fraction. However, since the upper critical magnetic field (H_{c2}) is higher than the lower critical magnetic field (H_{c1}) of Zn doped Bi-2223 sample, the loop does not collapse. The upper critical magnetic field (H_{c2}) and the lower critical magnetic field (H_{c1}) of Zn doped Bi-2223 sample were calculated from M-H loops at 10 K and found to be 8 and 0.12 Oe. Finally the magnetic susceptibility (χ) of Zn doped Bi-2223 samples were found to be -4.4146×10^{-5} .

Acknowledgements

We are grateful to Professor O.N. Srivastava and Professor R. S. Tiwari of the Department of Physics, B. H. U., Varanasi and Dr. G. D. Verma, Department of Physics, I.I.T., Roorkee for helpful and stimulated discussions.

References

1. Kamihara Y., Watanabe T., Hirano M. & Hosono H., *Journal of the American Chemical Society*, **2008**, 130, 3296.
2. Abd-Shukor R., & Kong W., *Journal of Applied Physics*, **2009**, 50, 07E311.
3. Ismail M., Abd-Shukor R., Hamadneh I. & Halim. S. A., *Journal of Materials Science*, **2004**, 39, 3517.
4. Lau KT, Yahya SY & Abd-Shukor R, *Journal of Applied Physics*, **2006**, 99, 123904.
5. Kuo Y. K., Schneider C. W., Nevitt M. V., Skove M. J. and Tessema G. X., *Phys. Rev. B*, **1997**, 63, 184515.
6. Bean C. P. *Phys. Rev. Lett.* **1962**, 8, 250.
7. Zeng D. C., Liu Z. Y., Zhou G. F., Wang Y. Z., de Boer F. R., Qiao G. W., *Journal of Applied Physics*, **2009**, 81, 4253.
8. Martin I, Balatsky A.V. and Zaanen J., *Physica C*, **2002**, 23, 69.
9. Nkum R.K., Punnett A. and Datars W.R., *Physica C*, **2002**, 38, 208.
10. Ling X. S., Park S. R., McClain B. A., Choi S. M., Dender D. C., and Lynn J. W., *Phys. Rev. Lett.* **2001**, 86, 712.
11. Ling X. S., Park S. R., Choi S. M., Dender D. C., and Lynn J. W., *Phys. Rev. Lett.* **2002**, 89, 259702.
12. Park S. R., Choi S. M., Dender D. C., Lynn J. W., and Ling X. S., *Phys. Rev. Lett.* **2003**, 91, 167003.
13. Dimitrov I. K., Daniilidis N. D., Elbaum C., Lynn J. W., and Ling X. S., *Phys. Rev. Lett.* **2007**, 99, 047001.
14. Daniilidis N. D., Park S. R., Dimitrov I. K., Lynn J. W., and Ling X. S., *Phys. Rev. Lett.* **2007**, 99, 147007.
15. Gammel P.L., Bishop D.J., Dolan G. J., Kwo J. R., Murray C. A., Schneemeyer L. F. and Waszczak J.V., *Phys. Rev. Lett.* **1987**, 59, 2592.
16. Gammel P.L., Schneemeyer L. F., Waszczak J. V. and Bishop D. J., *Phys. Rev. Lett.* **1988**, 61, 1666.

Advanced Materials Letters

Publish your article in this journal

[ADVANCED MATERIALS Letters](#) is an international journal published quarterly. The journal is intended to provide top-quality peer-reviewed research papers in the fascinating field of materials science particularly in the area of structure, synthesis and processing, characterization, advanced-state properties, and applications of materials. All articles are indexed on various databases including [DOAJ](#) and are available for download for free. The manuscript management system is completely electronic and has fast and fair peer-review process. The journal includes review articles, research articles, notes, letter to editor and short communications.

